RESEARCH ARTICLE

# Albumin binding and cytotoxicity assay of nickel oxide nanoparticles against primary hippocampal neural cells

***Sara Haji Hosseinali[1], Mojtaba Falahati[2]*, Pegah Ghoraeian[1]***

*[1]Department of Genetics, Faculty of Advanced Science and Technology, Tehran Medical Sciences, Islamic Azad University, Tehran, Iran*

*[2]Department of Nanotechnology, Faculty of Advanced Science and Technology, Tehran Medical Sciences, Islamic Azad University, Tehran, Iran*

**ARTICLE INFO**

***Article History:***
*Received 27 Oct 2019*
*Accepted 20 Dec 2019*
*Published 1 Feb 2020*

***Keywords:***
*Albumin*
*Cell Viability*
*Molecular Docking and Dynamics*
*Nickel Oxide*
*Nanoparticle*

**ABSTRACT**

Nanoparticles (NPs) have been widely used in medical and therapeutic applications. However, their albumin binding and their cytotoxicity assays have not been well explored. In his study, the interaction of NiO NPs with human serum albumin (HSA) was explored by circular dichroism (CD) study, molecular docking and dynamic studies. Afterwards the cytotoxicity of NiO NPs against primary hippocampal neural cells was explored by MTT and morphological assays. The CD experiment revealed that NiO NPs do not stimulate any significant structural changes within the HSA structure. The molecular docking investigation showed that NiO nanoclusters bind to HSA molecule through hydrophilic interactions and NiO nanoclusters with different sizes show different docking scores for interaction with HSA. The Molecular dynamic study also revealed that minor structural changes in HSA structure occur after interaction with NiO NPs. Cellular assay displayed that incubation of NiO NPs with primary hippocampal neural cells for 24 h triggered a significant cytotoxicity and morphological changes. Therefore, it may be concluded that although NiO NPs may show a strong binding affinity to HSA and do not induce a remarkable rearrangement in the structure of HSA, they may induce some unwanted effects on the cell viability

**How to cite this article**
*Haji Hosseinali S, Falahati M, Ghoraeian P. Albumin binding and cytotoxicity assay of nickel oxide nanoparticles against primary hippocampal neural cells. J. Nanoanalysis., 2020; 7(1): 1-9. DOI: 10.22034/jna.2019.1878049.1158*

## INTRODUCTION

NPs have been widely used in industry 1. and medicine 2., especially in imaging and drug delivery 3.. Indeed, NPs have been utilized for targeted drug delivery to CNS 4. as well as promising agents for imaging of different parts of brain 5., for example for drug delivery across the BBB 6.. Also, it has been demonstrated that NPs can be used for gene delivery 7. and siRNA delivery 8. to brain. In other side, NPs have been widely applied in tumour-specific therapy 9. and combined tumor imaging and therapy 10.

However, before medial utilization of NPs as drugs, their albumin binding and cytotoxicity should be evaluated. Because, HSA is known as a carrier protein and with its α-helical structure binds to different ligands such as drugs and NP and deliver them to the targeted cells. However, for potential binding of NPs to HSA, the biding affinity and preservation of the protein structure after interaction with NPs should be considered. Actually, understanding binding affinity, kind of interaction as well as structural changes of protein should be investigated upon interaction of proteins with NPs. Also, the interaction of NPs with cells should be assessed to explore the cytotoxicity effects of NPs against biological systems. It has been revealed that different NPs stimulate different kinds of cytotoxicity with several mechanisms. In other words, physicochemical properties of NPs can play a vital role in triggering the adverse effects of NPs and by changing these features, the cytotoxicity of

* Corresponding Author Email: *mojtaba.falahati@alumni.ut.ac.ir*

NPs can be minimized 11-14.. For example, it has been reported that NPs can trigger cytotoxicity against both normal and cancer cells 11, 12. It was revealed that $Al_2O_3$ NPs 13. and $CO_2O_3$ NPs 14. can induce cytotoxicity against neuron-like cells through elevation of apoptosis, cell cycle arrest, and apoptosis. In another studies, it was shown that ZnO NPs fabricated with biological routs can show anticancer and antibacterial activities 15.In some cases, it has been reported that the combination of NPs can play an important role in synergic cytotoxic effects on NPs against cancer cells 16..

Nickel oxide NiO NPs have been used as interesting materials in biomedical fields such as biosensors 17, 18., antibacterial and antiviral agents 19, 20., and anticancer drugs 21, 22.. Also, they have been used as contrasting materials in MRI and therapy of brain tumors 23, 24.. However, before the application of NiO NPs in medical areas, their toxicity and their ability to bind HSA molecules should be examined. Because, it has been revealed that these NPs may induce some structural changes within the biomolecules 25, 26. and stimulate cytotoxicity against normal cells 25, 26..

Therefore, in this study the structural changes of HSA in the presence of varying concentration of NiO NPs were explored by CD spectroscopy. Afterwards, the binding affinity and structural changes of HSA in the presence of NiO NPs was investigated by molecular docking and dynamic studies, respectively. Finally, the cytotoxicity of NiO NPs against primary neuron cells was assayed by cellular studies.

## MATERIALS AND METHODS

*Materials*

HSA lyophilized powder, Dulbecco's Modified Eagle's medium (DMEM), (3-(4,5-dimethylthiazol-2-yl)-2,5-diphenyltetrazolium bromide). (MTT), and NiO nanopowder (<50 nm) were purchased from Sigma-Aldrich Co., St. Louis, MO, USA. All other materials were of analytical grade and used without further purification. CD investigation was done at room temperature cylindrical cuvette using a Jasco CD spectropolarimeter (Aviv, 215Model, USA).

*Methods*

*Sample preparation*

HSA and NiO NPs with defined concentrations were dissolved in phosphate buffer (pH 7.4, 10 mM). NiO NPs were also vortexed and incubated in the water bath at 55°C for 30 min.

*Circular dichroism study*

The obtained spectra were subtracted against baseline and NP noise, and final ellipticities spectra were captured at a scan rate of 10 nm $min^{-1}$ from 200 to 250 nm. The MRE of HSA either alone or in the presence of different doses of NiO NPs (0.01, 0.05, 0.1, and 0.2 mg/ml) were calculated. The MRE data were utilized to estimate the secondary structural changes of HSA.

*Molecular docking and dynamic methods*

Three spherical clusters with diameter of 1, 3, 5 nm were constructed by repeating NiO unit cells and used as models of NiO NPs in the simulations. The X-ray crystallographic 3D structure of HSA (PDB ID: 1AO6) was downloaded from the online Protein Data Bank RCSB PDB (http://www.pdb.org). Molecular docking investigation was carried out by HEX 6.3 software 27.. Visualization of the interacting site was done by using CHIMERA (www.cgl.ucsf.edu/chimera) and PyMOL (http://pymol.sourceforge.net/) tools. The molecular dynamics simulations have been performed using the Forcite code and universal force field (UFF) 28..

*Neural primary cells culture*

Primary neural cells were dissociated from embryonic mice by cervical dislocation based on the previous report done by Kamran Khalid et al., 29.. Briefly, after isolation of hippocampi, enzymatic digestion was done. This process was followed by separation of the neural cells in serum-containing medium and seeding onto 96-well plates in 250 µL DMEM per well added by other necessary supplements. After incubation (2 h), the medium was gently removed and replaced by the pre-warmed neurobasal medium. The cells were finally incubated at 37 °C in 5% $CO_2$ humidified atmosphere for 14 days before addition of NPs.

*MTT assay*

MTT assay was done to examine the cell mortality in the presence of varying concentrations of NiO NPs (1-200 µg/ml). The cells ($1\times10^4$ cells) were seeded onto 96-well plates and different concentrations of NiO NPs (1, 10, 50, 100, and 200 µg/ml) were added to the cells and then incubated in for 24 h. Afterwards, MTT solution (0/5 mg/mL) was added to each well and incubated for 4 h. Then, the media were gently removed and 100 µl

DMSO was added for 2 min. The cell viability was then calculated by the optical density read at 570 nm using ELISA reader (Expert 96, Asys Hitch, Ec Austria).

*Morphological changes assay*

The morphological changes of primary neurons in the presence of $IC_{50}$ concentration of NiO NPs after 24 h was assessed by inverted microscope (Zeiss, Germany).

*Statistical analysis*

Statistical analysis was performed using ANOVA followed by Dunn's post hoc tests for pairwise comparisons with the negative control group. *P-value<0.5 was used as a significance between treated and control groups.

## RESULTS AND DISCUSSION

*NiO NP characterization*

NiO NPs were fully characterized by TEM and DLS in our previous paper 25, 26.. DLS study showed that the NiO NPs have a hydrodynamic radius and zeta potential value of around 90 nm and -30 mV, respectively 25.. TEM investigation also revealed that the NiO nanopowder has a size of around 50 nm 26.

*Circular dichroism study*

CD study can be utilized to explore the secondary structural changes of protein after interaction with NPs 11, 13.. In this study, Far UV-CD was utilized to reveal the secondary structural changes of HSA after interaction with different concentrations (0.01, 0.05, 0.1, and 0.2 mg/ml) of NiO NPs. As shown in Fig. 1, HSA molecule shows two minima set at 208 nm and 222 nm, indicating the predominance of α-helical structure in the HSA conformation 25.. Also, it was deduced that after addition of different concentrations of NiO NPs, the ellipticity variations around 208 nm and 222 nm are almost unchanged. This data indicated that the secondary structural changes of HSA in the presence of NiO NPs was a type of minor rearrangement. Therefore, it may be concluded that NiO NPs induce some minor secondary structural changes within the HSA conformation.

*Molecular docking study*

Indeed, the molecular docking study can be employed to provide detail information about the interaction between a small molecule like a NP and a biomolecule (protein) at the sub-molecular level, which result in characterization of the behavior of NPs in the interacting site of target molecules as well as to explore basic biological processes 30, 31.. Therefore, in this study, the interaction of spherical NiO nanoclusters with different sizes of 1 nm (Fig. 2a), 3 nm (Fig. 2b), and 5 nm (Fig. 2c) and HSA was investigated by docking software (HEX 6.3). As shown in Fig. 2, the designed nanoclusters bind to different poses on the HSA structure, indicating the effect of sizes on the binding affinity of NPs and proteins.

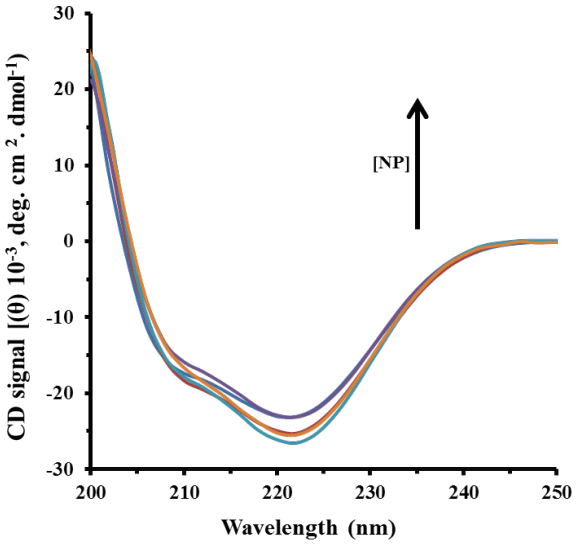


Fig. 1. CD spectra of HSA alone (light blue), and HSA in the presence of varying concentrations of NiO NPs 0.01 µg/ml (red), 0.05 µg/ml (orange), 0.1 µg/ml (dark blue), and 0.2 µg/ml (purple). CD experiment was done at room temperature and the phosphate buffer, pH 7.4, 10 mM) was used as a solvent to prepare protein and NiO NP solution. The CD spectra were corrected automatically against buffer and NP solutions.

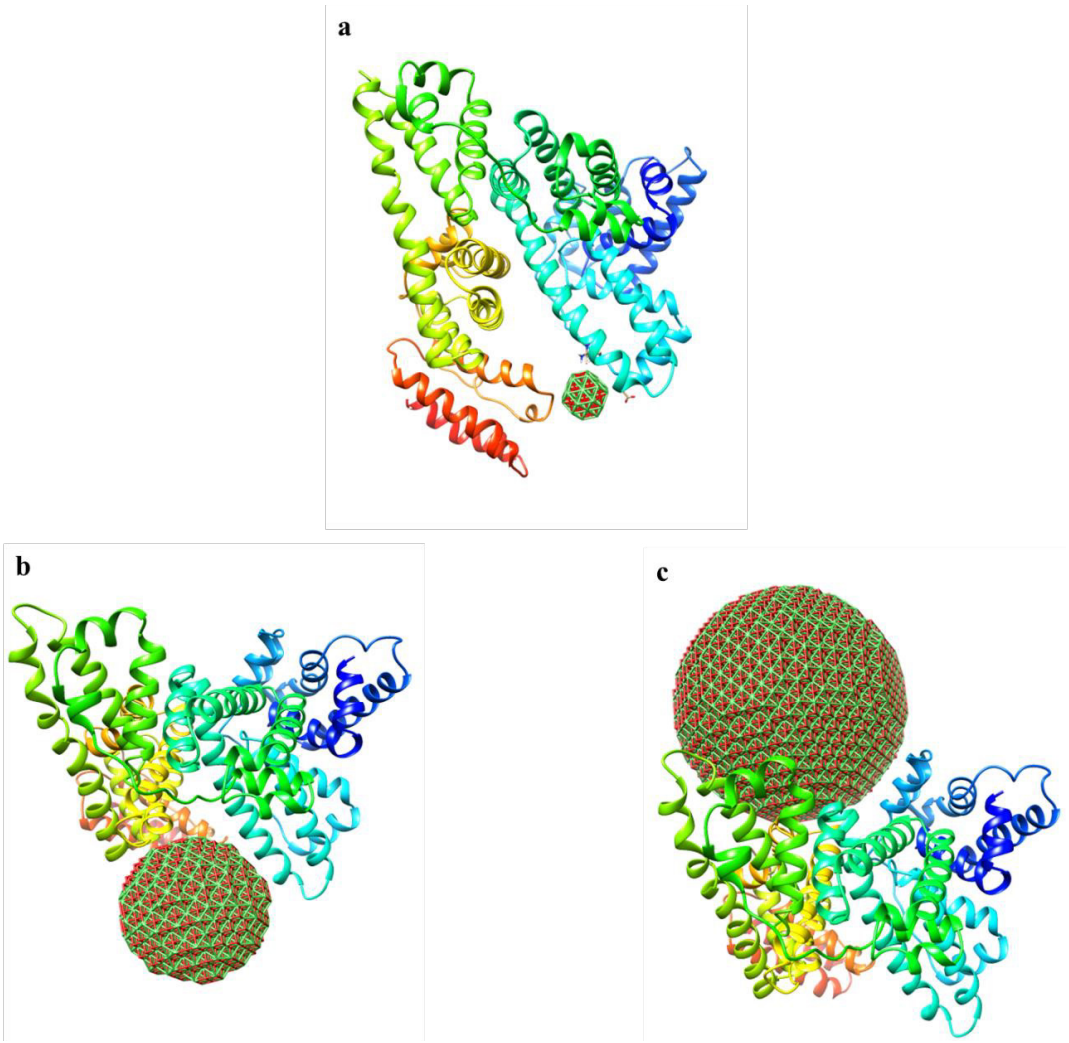


Fig. 2. Interaction of HSA with NiO nanoclusters investigated by HEX 6.3 software. NiO nanocluster with different sizes of 1nm (a), 3 nm (b), and 5 nm (c).

To explore the affinity of different clusters with HSA, docking score was calculated. As summarized in Table 1, it can be deduced that NiO nanoclusters with different sizes of 1 nm, 3 nm, and 5 nm show different docking scores of -161.70, -474.52, and -134.34 E-values, respectively. Therefore, it can be suggested that the affinity of NiO nanocluster toward HSA molecules with a size of 3 nm is the highest among other sizes of NPs.

Table 1. Docking scores of NiO clusters with HAS

| NP | Diameter | Docking score (E-value) |
|---|---|---|
| **NiO** | 1 nm | -161.70 |
| **NiO** | 3 nm | -474.52 |
| **NiO** | 5 nm | -134.34 |

The visualization of docked pose was done by PyMOL and CHIMERA tools to obtain detailed data about the residues involved in the binding site between nanocluster and HSA. Fig.3 shows the residues interacted with NiO nanoclusters with different sizes of 1nm (Fig.3a), 3 nm (Fig.3b), and 5 nm (Fig.3c). It can be seen that different residues establish different connections between HSA and nanoclusters. The interacted residues between HSA molecule and NiO nanoclusters are tabulated in Table 2.

As NiO nanocluster with a size of 3 nm shows the highest affinity to HSA molecule, it can be revealed that Lys-439, Gly-434, Ser-435, Phe-395, Glu-396. Gly-399, Glu-400, Lys-402, Tyr-401, Lys-519, Gln-522, GLu-518, Leu-179, Asp-183, Glu-

Table 2. Docking scores of NiO clusters upon interaction with HAS

| NP | Diameter | Residue interacted |
|---|---|---|
| **NiO** | 1 nm | Val-116, Arg-117, Glu-119, Leu-516, Thr-515 |
| **NiO** | 3 nm | Lys-439, Gly-434, Ser-435, Phe-395, Glu-396. Gly-399, Glu-400, Lys-402, Tyr-401, Lys-519, Gln-522, GLu-518, Leu-179, Asp-183, Glu-184 |
| **NiO** | 5 nm | Lys-93, Asp-89, Glu-86, Gln-104, Lys-205, Lys-466, Glu-465, Thr-478, Thr-474, Lys-475, Asp-471, Val-469, Pro-466 |

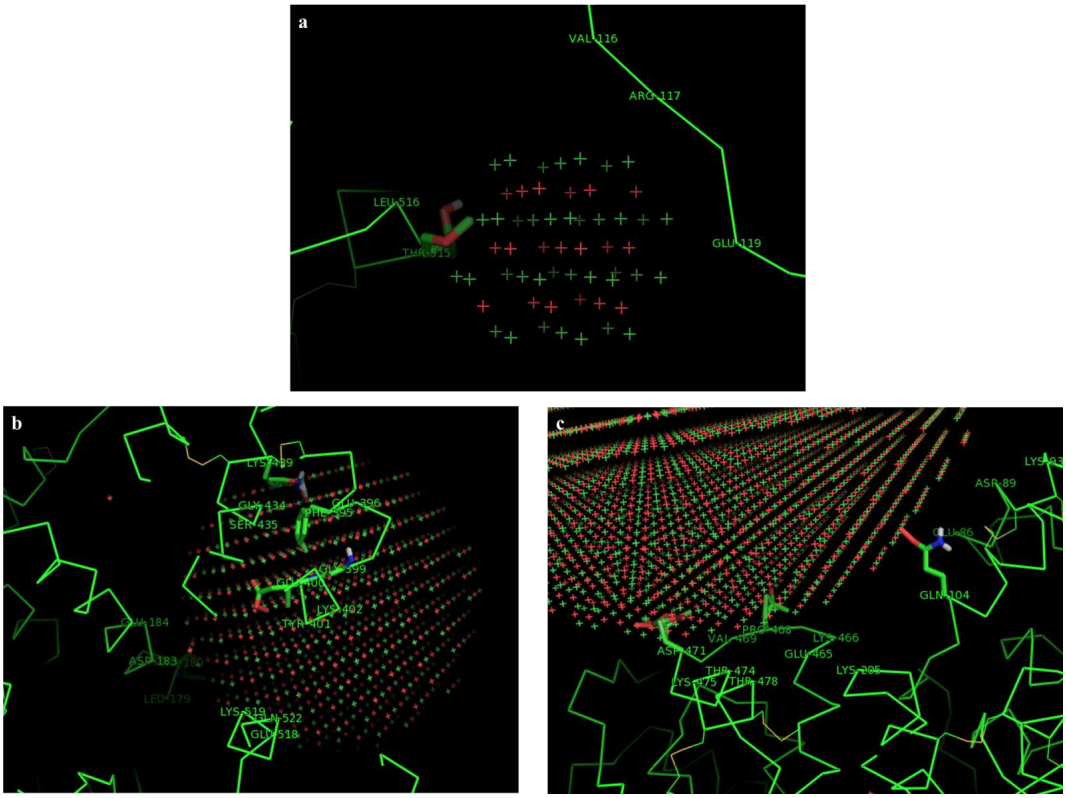


Fig. 3. The output form PyMOL and CHIMERA tools for visual screening of docked pose between HSA and NiO nanoclusters with different sizes of 1nm (a), 3 nm (b), and 5 nm (c).

184, are the preferred residues for the interaction of NiO nanocluster with HSA molecules. Indeed, it can be concluded that NiO NPs interacted with HSA molecules through hydrophilic forces.

Therefore, docking process help us to predict the NP position and its spatial orientation within the docked pose and assess the binding affinity. Revealing the position of the binding site remarkably enhance the predicting the experimental outcomes.

*Molecular dynamics study*

Molecular dynamics study can provide data regarding the conformational changes of proteins after interaction with ligands like NPs 32, 33.. Material Studio software can be used to reveal structural changes within proteins.

The earliest explanation for the NP-protein binding affinity and related structural changes of proteins can provide useful information about the active site of the protein as well as revealing some information about the rearrangement of the protein structure induced by interactions with the NPs.

The microcanonical ensemble with a time step of 1 fs, and a total simulation time of 500 ps, were utilized in the molecular dynamics simulation. A cluster with a diameter of 3 nm and one chain

of albumin were used in the molecular dynamics simulation. Fig.4 shows the adsorbed protein on NiO nanocluster with a size of 3 nm before (Fig.4a) and after evolution (Fig 4.b). As can be seen the protein slightly reshaped after the evolution. In other word, protein may be subjected to some minor conformational changes after interaction with NiO NPs, which is in good agreement with CD data.

NPs can induce some unwanted impacts against biological systems. These adverse effects should be examined *in vitro* before their application *in vivo*. In this paper, it was depicted that NiO NPs can bind to HSA molecules though hydrophilic interactions and do not stimulate the protein denaturation. This effect can be considered as a promising application of NiO NPs in pharmaceutical fields. Because, HSA molecules as a carrier protein should not lose their structure after interaction with a NPs. In accordance with our data, it has been shown that interaction of fullerene 34. and copper oxide NPs 35. with albumin induced no significant structural changes in the protein structure. However, it has been reported that other NPs such as $Fe_2O_3$ NPs 36., ZnO NPs 37., $Al_2O_3$ NPs 38., Au NPs 39., Ag NPs 40., and QDs NPs 41. upon interaction with albumin induced some substantial structural changes.

*MTT assay*

Primary neural cells seeded in a 96-well plate were incubated with NiO NPs at different concentrations (1, 10, 50, 100, and 200 µg/mL) for 24 h. As shown in Fig. 5, at lower concentrations of 1 and 10 µg/ml, the cell viability rates for 24 h incubation were 96.93% and 93.31%, respectively. Interestingly, at a higher concentration of 50 and 100 µg/ml, the cell viability rates after 24 h incubation were reported to be 74.76% (*P-value<0.05) and 59.16% (*P-value<0.05), respectively. Moreover, at further higher concentrations of 200 µg/ml, the cell mortality was more induced in the 24 h incubation group. At the highest concentration of 200 µg/ml, the cell viability was 32.54% for 24 h incubation. When compared to negative control group, 24 h incubations with the highest dose (200 µg/ml) caused a remarkable reduction in viability (**P-value<0.01). The $IC_{50}$ concentration of NiO NPs against primary neurons was calculated to be around 120 µg/ml.

*Morphological assay*

Morphological analysis of cells using inverted microscopy was done after 24 h incubation of cells with $IC_{50}$ concentration (120 µg/ml) of NiO NPs. As shown in Fig. 6a, control cells show no significant morphological changes and have long axons with round shaped soma. However, after adding of NPs, remarkable morphological differences in cells were observed relative to the negative control cells, specifically, significant axon changes, e.g. axon

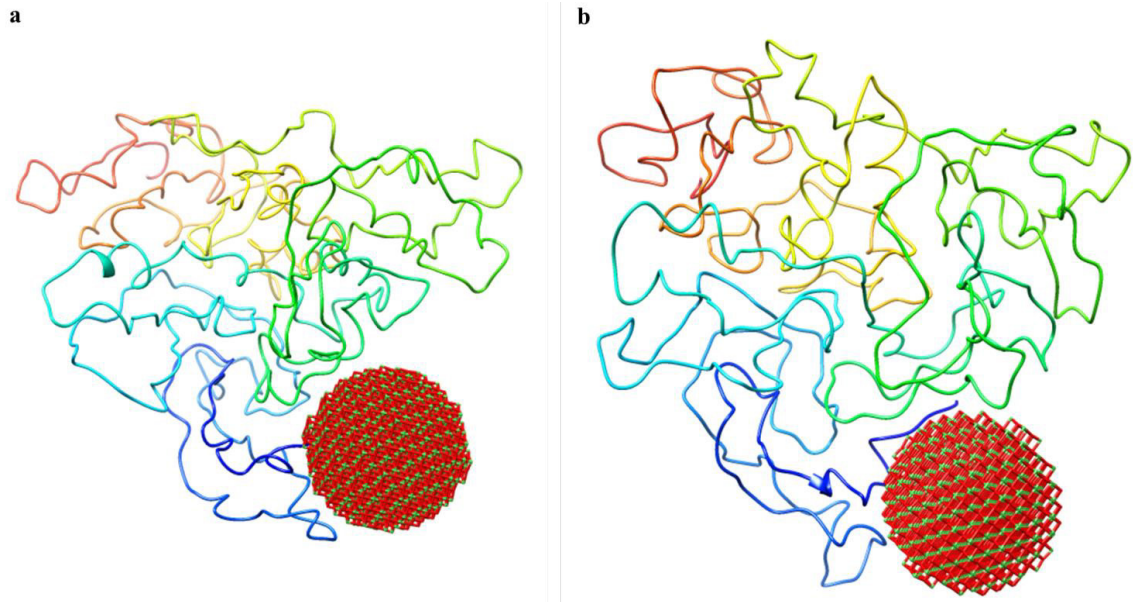


Fig. 4. The molecular dynamic simulation of HSA molecule (one subunit) with NiO nanocluster (3 nm) in the beginning (a) and after total simulation time of 500 ps (b).

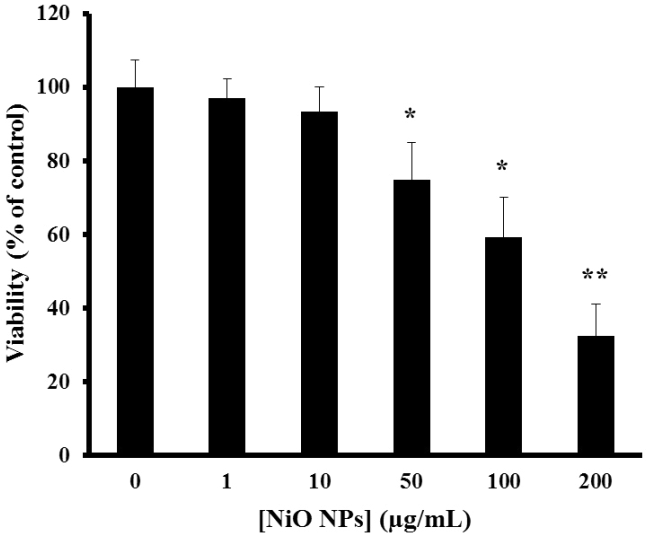


Fig. 5. The effects of NiO NPs on the viability of primary neuron cells, determined by MTT assay. Statistical analysis showed that 24 h incubation with 50 µg/mL and 100 µg/mL NiO NPs significantly decreased the cell viability as compared to negative control cells (* P-value < 0.05). In the case of cells treated with 200 µg/ml NiO NPs, cell viability was significantly reduced at a higher rate (**P-value < 0.01).

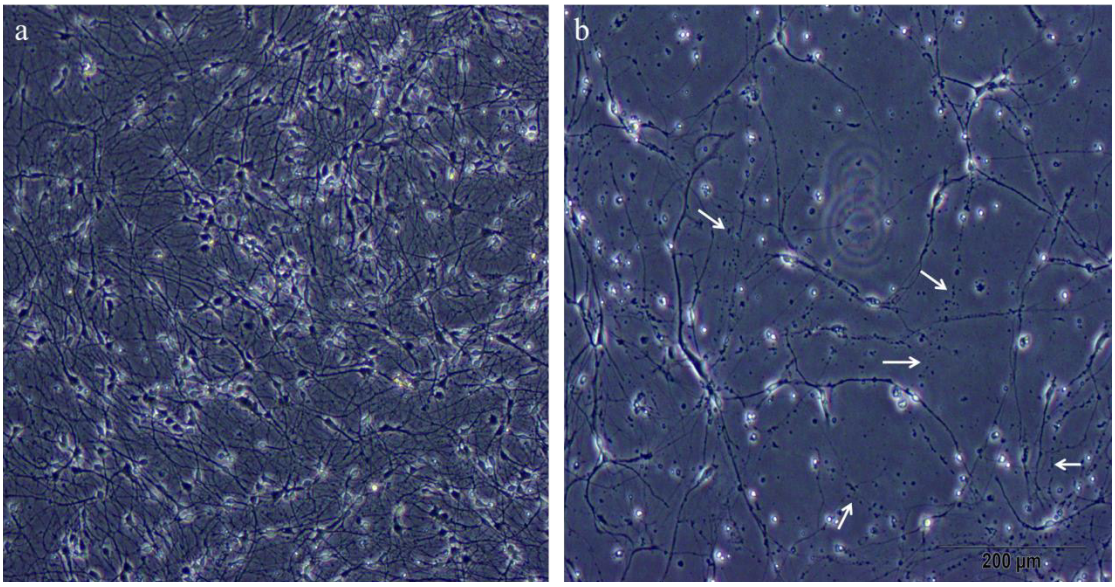


Fig. 6. The effects of $IC_{50}$ concentration of NiO NPs on the morphological changes of primary neuron cells, determined by inverted microscope. Control cells (a) and treated cells with $IC_{50}$ concentration of NiO NPs (b). The arrows show the fragmented axons.

fragmentation (Fig. 8b).

Regarding cellular assays, it was shown that NiO NPs stimulated a significant cell mortality and axon fragmentation in primary hippocampal neural cells. Similar to our results, Lai et al., 42. revealed that titanium dioxide NPs incubation with cells resulted in induction of cytotoxicity on human neural cells and fibroblasts. Furthermore, Ngwa et al., displayed that manganese NPs resulted in activation of apoptotic signaling and autophagy in dopaminergic neuronal cells 43.

Also, Valdiglesias et al., 44. showed that ZnO NPs also triggered neuronal toxicity and genotoxicity in a dose-dependent manner. Moreover, Chaing et al., 45. reported that ZnO NPs triggered toxicity and DNA damage in rat primary neuronal cells. Haase

et al., 46. also depicted that silver NPs can cross the primary mixed neural cells and increase the production of a significant level of free radicals and acute calcium responses in treated cells. In another study, Costa at al., revealed that superparamagnetic $Fe_2O_3$ NPs stimulated cell mortality on neuronal and glial cells 47.. Recently, several reports have been shown that $SiO_2$ NPs 48., Au NPs 49. and magnetic Ni ferrite NPs 50. can trigger a significant cytotoxicity on neural cells.

Therefore, it may be concluded that the type of NPs determine the kind of interaction between NPs and proteins or cells and these interactions play a pivotal role in determining the severity of protein denaturation or cytotoxicity.

## CONCLUSION

In this paper the interaction of NiO NPs with HSA and primary neuron cells was explored by different spectroscopic, theoretical and cellular methods. It was shown that, although NiO NPs bind to HSA with strong bonds and do not stimulate significant structural changes within the protein structure, they may induce some remarkable cytotoxicity effects. Therefore, it may be suggested that for screening the toxicity of NPs, several approaches should be used to point out the adverse effects of NPs on the biological systems.

## ABBREVIATION

Alumina: $Al_2O_3$; Blood brain barrier: BBB; Dynamic light scattering: DLS; Central nervous system: CNS; Circular dichroism: CD; Human serum albumin: HSA; Mean residue ellipticities MRE; Quantum dots: QDs

## ACKNOWLEDGMENT

We must acknowledge the financial support received from the Tehran Medical Sciences, Islamic Azad University.

## CONFLICT OF INTEREST

The authors declare that there is no conflict of interests regarding the publication of this manuscript.

## REFERENCES

1. C. Gaylarde and B.O. Ortega-Morales, Archives Of Nanomedicine: Open Access Journal,1,10, (2018).
2. A. Kermanizadeh , L.G. Powell, V. Stone and P Møller, International journal of nanomedicine. 13, 7575, (2018)
3. D.Vinciguerra, S. Denis, J. Mougin , M. Jacobs, and J. Nicolas, Journal of controlled release. 28, 425, (2018)
4. P. Henrich-Noack, S. Prilloff, N. Voigt , J. Jin , W. Hintz , J. Tomas and B.A. Sabel, Archives of toxicology, 86,1099, (2012).
5. A. Meola, J. Rao, N. Chaudhary, M. Sharma and S.D. Chang, 9,1, (2018).
6. Y. Zhou, Z. Peng, E.S. Seven ES and R.M. Leblanc, Journal of controlled release, 270, 290, (2018)
7. G. Erel-Akbaba, L.A. Carvalho, T. Tian, M. Zinter and B.A. Tannous, ACS Nano, 13, 4028, (2019)
8. M. Zheng, W. Tao, Y. Zou, O.C. Farokhzad and B. Shi, 36, 562, (2018)
9. H. Lin, Y. Chen and J. Shi, Chemical Society Reviews, 47,1938, (2018)
10. Y. Hu, S. Mignani, J.P. Majoral, M. Shen and X. Shi, Chemical Society Reviews, 47, 1874, (2018)
11. S.T. Kim, K. Saha, C. Kim and V.M. Rotello, Accounts of chemical research. 46, 681, (2013)
12. A. Morovati, S. Ahmadian and H. Jafary, Molecular biology reports, 5, 7, (2019)
13. Z.R. Kermani, S.S. Haghighi and M. Falahati, International journal of biological macromolecules, 120, 1140, (2018)
14. M. Nouri and M. Falahati, International journal of biological macromolecules. 118, 1763, (2018)
15. A. Hussain and I. Ali, RSC Advances. 9, 15357, (2019)
16. A. Neshastehriz, Z. Khosravi, H. Ghaznavi and A. Shakeri-Zadeh, Radiation and environmental biophysics. 57, 405, (2018)
17. X. Zhuang, C. Tian, F. Luan, X. Wu and L. Chen, RSC Advances, 6, 9254i, (2016)
18. W. Dai and B. Yang, Electrochimica Acta, 187, 413, (2016)
19. M. I. Din, A. G. Nabi, A. Rani, A. Aihetasham and M. Mukhtar, Environmental Nanotechnology, Monitoring & Management. 9, 29, (2018)
20. A. A. Ezhilarasi and H. A. Al-Lohedan, Journal of Photochemistry and Photobiology B: Biology. 180, 39, (2018)
21. S. Bano, S. Nazir, S. Munir, M.F. AlAjmi, M. Afzal and Mazhar, International journal of nanomedicine. 11, 3159, (2016)
22. S. Khan and A. A. Khan, Journal of Trace Elements in Medicine and Biology. 52, 12, (2019)
23. M. Wankhede, A. Bouras, M. Kaluzova and C. G. Hadjipanayis, Expert review of clinical pharmacology. 5, 173, (2012)
24. M. A. Shevtsov, International journal of nanomedicine, 9, 273, (2014)
25. M. Hajimohammadjafartehrani, S.H. Hosseinali, A. Dehkohneh, P. Ghoraeian, M. Ale-Ebrahim, K. Akhtari, K. Shahpasand, A.A. Saboury, F. Attar and M. Falahati, International journal of biological macromolecules. 127, 330, (2019)
26. S.H. Hosseinali, Z.P. Boushehri, B. Rasti, M. Mirpour, K. Shahpasand and M. Falahati, International journal of biological macromolecules. 15, 125, (2019)
27. D.W. Ritchie and V. Venkatraman, Bioinformatics. 26, 2398, (2010)
28. C.J. Casewit and W.M. Skiff , J Am Chem. Soc. 114, 10024, (1992)
29. M. Khalid M, International journal of molecular sciences, 19, 2613, (2018)
30. S. Nourizadeh and S. Abbasi, Journal of fluorescence. 28, 551, (2018)
31. Q. Sun , H. Yang, P. Tang, J. Liu, W. Wang and H. Li, Food

chemistry, 15, 243, (2018)
32. S.Q. Yesylevskyy , C. Ramseyer, M. Savenko, S. Mura and P. Couvreur, Molecular pharmaceutics, 15, 585, (2018)
33. S. Moradi, M. Taran M, and M. Shahlaei, International journal of biological macromolecules. 107, 2525, (2018)
34. S. Liu, Y. Sui, K. Guo, Z. Yin and X. Gao, Nanoscale research letters, 7, 433, (2012)
35. P. Esfandfar, M. Falahati and A. Saboury, Journal of Biomolecular Structure and Dynamics. 34, 1962, (2016)
36. Q. Yang, J. Liang and H. Han, The Journal of Physical Chemistry B., 113, 10454, (2009)
37. A. Bhogale and D.C. Kothari, Colloids and Surfaces B: Biointerfaces. 102, 257, (2013)
38. A. Rajeshwari and A. Mukherjee, Journal of Luminescence, 145, 859, (2014)
39. G. Mandal, M. Bardhan and T. Ganguly, Colloids and Surfaces B: Biointerfaces. 81, 178, (2010)
40. M.S. Ali, H.A. Al-Lohedan, A.M. Atta, A.Q. Ezzat and S.A. Al-Hussain, Journal of Molecular Liquids, 204, 248, (2015)
41. L. Lai and Y. Liu, Spectrochimica Acta Part A: Molecular and Biomolecular Spectroscopy. 97, 366, (2012)
42. J.C. Lai and S.W. Leung, International journal of nanomedicine. 3, 533, (2008)
43. H.A. Ngwa, A. Kanthasamy, Y. Gu, N. Fang, V. Anantharam and A.G. Kanthasamy, Toxicology and applied pharmacology. 256, 227, (2011)
44. V. Valdiglesias and J.P Teixeira, Environment international, 55, 92, (2013)
45. H.M. Chiang and P.P. Fu, Journal of nanoscience and nanotechnology,12, 2126, (2012)
46. A. Haase and G. Reiser, Toxicological sciences, 126, 457, (2012)
47. C. Costa and B. Laffon, Journal of Applied Toxicology, 36, 361, (2016)
48. Y. Kamikubo, T. Yamana, Y. Hashimoto and T. Sakurai, ACS chemical neuroscience. 19, 304, (2018)
49. T.A. Mishchenko and V.M. Vedunova, KnE Energy, 2, 232, (2018)
50. M. Amiri, A. Pardakhti, M. Ahmadi-Zeidabadi, A. Akbari and M. Salavati-Niasari, Colloids and Surfaces B: Biointerfaces. 172, 244, (2018)